MEDICAL SCIENCES

Correction for "Genetic inactivation of AKT1, AKT2, and PDPK1 in human colorectal cancer cells clarifies their roles in tumor growth regulation," by Kajsa Ericson, Christine Gan, Ian Cheong, Carlo Rago, Yardena Samuels, Victor E. Velculescu, Kenneth W. Kinzler, David L. Huso, Bert Vogelstein, and Nickolas Papadopoulos, which appeared in issue 6, February 9, 2010, of *Proc Natl Acad Sci USA* (107:2598–2603; first published January 20, 2010; 10.1073/pnas.0914018107).

The authors note that all columns and error bars in their figures represent means and SDs.

www.pnas.org/cgi/doi/10.1073/pnas.1002415107

NEUROSCIENCE

Correction for "Subregional neuroanatomical change as a biomarker for Alzheimer's disease," by Dominic Holland, James B. Brewer, Donald J. Hagler, Christine Fenema-Notestine, Anders M. Dale, and the Alzheimer's Disease Neuroimaging Initiative, which appeared in issue 49, December 8, 2009, of *Proc Natl Acad Sci USA* (106:20954–20959; first published November 20, 2009; 10.1073/pnas.0906053106).

The authors note that the author name Christine Fenema-Notestine should have appeared as Christine Fennema-Notestine. The corrected author line appears below. The online version has been corrected.

Dominic Holland[a,1], James B. Brewer[a,b], Donald J. Hagler[b], Christine Fennema-Notestine[b,c], Anders M. Dale[a,b], and the Alzheimer's Disease Neuroimaging Initiative[2]

www.pnas.org/cgi/doi/10.1073/pnas.1001505107

EDITORIAL EXPRESSION OF CONCERN. PNAS is publishing an Editorial Expression of Concern regarding the following two articles:

(*i*) BIOPHYSICS. "Structure of vaccinia complement protein in complex with heparin and potential implications for complement regulation," by Vannakambadi K. Ganesh, Scott A. Smith, Girish J. Kotwal, and Krishna H. M. Murthy, which appeared in issue 24, June 15, 2004, of *Proc Natl Acad Sci USA* (101:8924-8929; first published June 3, 2004; 10.1073/pnas.0400744101).

(*ii*) BIOPHYSICS. "Crystal structure of human apolipoprotein A-I: Insights into its protective effect against cardiovascular disease," by A. Abdul Ajees, G. M. Anantharamaiah, Vinod K. Mishra, M. Mahmood Hussain, and H. M. Krishna Murthy, which appeared in issue 7, February 14, 2006, of *Proc Natl Acad Sci USA* (103: 2126-2131; first published February 1, 2006; 10.1073/pnas.0506877103).

The editors wish to note that we have received a report from the University of Alabama at Birmingham (UAB) that has investigated allegations of falsified or fabricated protein crystallographic structures including PDB codes 1RID and 2A01, which were published in the PNAS papers noted above. The UAB committee has forwarded their findings to the US Office of Research Integrity (ORI). We are awaiting the findings of ORI to determine the appropriate next steps.

Randy Schekman
Editor-in-Chief

www.pnas.org/cgi/doi/10.1073/pnas.1003210107

Retraction

BIOPHYSICS

Retraction for "Structure of vaccinia complement protein in complex with heparin and potential implications for complement regulation," by Vannakambadi K. Ganesh, Scott A. Smith, Girish J. Kotwal, and Krishna H. M. Murthy, which was first published June 3, 2004; 10.1073/pnas.0400744101 (*Proc Natl Acad Sci USA* 101:8924–8929).

The US Office of Research Integrity has found that Krishna H. M. Murthy falsified and/or fabricated the protein crystal structure of vaccinia virus complement control protein in complex with heparin reported in this article and the corresponding structure factors and coordinate file deposited in the Protein Data Bank for entry 1RID (1). Accordingly, PNAS is retracting the article.

1. *Federal Register* 83 (2018), pp 16370–16371. Available at https://www.federalregister.gov/d/2018-07782. Accessed June 8, 2018.

Published online July 9, 2018.

www.pnas.org/cgi/doi/10.1073/pnas.1806429115

RETRACTION

Structure of vaccinia complement protein in complex with heparin and potential implications for complement regulation

Vannakambadi K. Ganesh*, Scott A. Smith†, Girish J. Kotwal†‡, and Krishna H. M. Murthy*§

*Center for Biophysical Science and Engineering, University of Alabama at Birmingham, Birmingham, AL 35294-4400; †Department of Microbiology and Immunology, University of Louisville School of Medicine, Louisville, KY 40202; and ‡Division of Medical Virology and Institute for Infectious Diseases and Molecular Medicine, University of Cape Town, HSC, Cape Town, South Africa 7925

Edited by Timothy A. Springer, Harvard Medical School, Boston, MA, and approved May 4, 2004 (received for review February 2, 2004)

Vaccinia virus complement control protein (VCP), a homolog of the regulators of the complement activation family of proteins, inhibits complement activation through mechanisms similar to human fluid-phase complement regulators factor H and C4b-binding protein. VCP has a heparin-binding activity that assists vaccinia in host interactions. Interaction with cell-surface polyanions like heparin is centrally important in the functioning of fluid-phase complement regulators and is the basis of host-target discrimination by the alternative pathway. We report the structure of VCP in complex with a heparin decasaccharide, which reveals changes in VCP that might be pertinent to complement regulation. Properties that VCP shares with fluid-phase complement regulators suggest that such conformational changes may be of relevance in the functioning of other complement regulators. Additionally, comparison of VCP–heparin interactions with potentially similar interactions in factor H might enable understanding of the structural basis of familial hemolytic uremic syndrome, attributed to mutational disruption of heparin and C3b binding by factor H.

Vaccinia virus complement control protein (VCP) is a homolog of the members of the regulators of complement activation family and aids the virus in evading the complement-mediated inflammatory response in the host (1, 2). VCP down-regulates both the classical pathway (CP) and the alternative pathway (AP) of complement by inhibition of C3 and C5 convertases through interaction with C3b and C4b, in a manner analogous to that of membrane cofactor protein (MCP/CD46), decay acceleration factor (DAF/CD55), factor H (FH), and C4b-binding protein (C4BP) (3–5). Therapeutic exploitation of the host complement regulatory mechanisms, through development of vaccines that enhance AP activation (6) and of antibiotics that render microbes more vulnerable to complement attack (7), has been proposed. Conversely, suppression of complement activation, through use of soluble versions of human MCP, DAF, and complement receptor type 1 (CR1), has been sought in many conditions where inappropriate complement activation endangers the host, including hyperacute rejection of xenogeneic transplants, ischemia–reperfusion injury, Alzheimer's disease, biomaterial incompatibility injury, restenosis, and systemic lupus erythematoses (8). Although soluble forms of human regulators, due to their potential lack of immugenicity in humans, have shown the most promise (8), small size, ability to down-regulate both pathways, capacity to work in the fluid phase as well as when bound to cell surfaces, intrinsic solubility, and thermal stability, leading to suggestions that VCP might also possess significant potential for clinical use (4, 9).

Regulators of complement activation proteins are composed, partly or wholly, of 60 residue disulfide-bonded segments called short consensus repeats (SCRs, or complement control modules) (10). FH and C4BP, the primary regulators of the alternative and classical pathways, respectively, are large glycosylated proteins, the former made up of 20 SCRs and the latter of 7 chains each with 8 SCRs (11, 12). Structures of several complement regulators have been reported and have significantly assisted in elucidation of structure–function relations. These include fragments of FH and VCP (reviewed in ref. 13); two of four SCRs in MCP (CD46) that serve as a measles virus receptor (14); a three-SCR fragment from CR1 (CD35), which contains its C3b-binding site (15); a functionally important DAF fragment (16); as well as SCRs that form parts of other complement components such as C1s (17). Some of the critical structural interactions involved in the binding of a two-SCR fragment of CR2 (CD21) with its C3d ligand have also been recently revealed (18). Structural information on FH and C4BP has been more difficult to obtain because of their large size, extensive glycosylation, and intermodular flexibility. However, VCP, which consists of just four SCRs and has functional properties similar to both FH and C4BP, has proven to be an informative model for the elucidation of structure–function relations in complement regulators (13, 19). A key property that VCP shares with FH and C4BP is the ability to bind heparin (20–22). Binding of VCP to heparin or other glycosaminoglycans is postulated to play a crucial role in the vaccinia infection cycle, enabling the virus to prolong its residence in host cells, modify host chemokine response, and gain protection from the host immune response (23). The structure of VCP allowed us to identify, through molecular modeling, two putative heparin-binding sites based on geometric similarity to that in acidic fibroblast growth factor (FGF1) (19, 24). Subsequent studies indicated that the site identified on SCR4 had probable biological relevance (5). Interaction between polyanions, such as heparin, and FH plays a critical role in target recognition and self/nonself distinction made by the AP (25). Recent genetic studies have correlated inadequacies in heparin and C3b binding by FH as the probable cause of familial hemolytic uremic syndrome (HUS) in humans (26, 27). Characterization of the structural details of heparin interaction with complement regulators thus has the potential of significantly enhancing the understanding of the regulation of AP activation, the underlying structural defects in HUS, and the vaccinia infection cycle. Although interactions of complement regulators with heparin have been the objects of many modeling studies (19, 28–30), there is currently no experimentally determined structure of a complement regulator bound to heparin. We report the structure of VCP complexed with a heparin decamer fragment determined at 2.1 Å. The conformational changes observed in heparin-bound VCP might have relevance

This paper was submitted directly (Track II) to the PNAS office.

Abbreviations: VCP, vaccinia virus complement control protein; AP, alternative pathway; MCP, membrane cofactor protein; DAF, decay acceleration factor; FH, factor H; C4BP, C4b-binding protein; SCR, short consensus repeat; FGF, fibroblast growth factor; HUS, hemolytic uremic syndrome; SPICE, smallpox inhibitor of complement enzymes.

Data deposition: The atomic coordinates have been deposited in the Protein Data Bank, www.pdb.org (PDB ID code 1RID).

§To whom correspondence should be addressed. E-mail: murthy@cbse.uab.edu.

www.pnas.org/cgi/doi/10.1073/pnas.0400744101

Table 1. Data measurement and structure refinement

Data measurement	
Cell, Å and degree	$a = 60.71$; $b = 76.98$ $c = 116.74$; $\beta = 91.2$
Space group	P2
Copies in AU	2
Maximum resolution, Å*	2.1 (2.19–2.1)
Measured reflections,* %	98 (90)
R_{merge}†	0.047 (0.104)
$\langle I/\sigma I \rangle$	16.2 (8.7)
⟨Redundancy⟩	3.3 (2.2)
Refinement and geometry	
R_{cryst}*	0.207 (0.282)
R_{free}*	0.247 (0.309)
Bond rms deviation, Å	0.015
Angle rms deviation degrees	1.4
Ramachandran outliers	0
Current model	
Protein atoms (⟨B⟩)	3,715 (29.7)
Heparin	274 (38.6)
Water oxygen	821 (48.5)

*Values for highest-resolution shell are given in parentheses.
†$R_{merge} = \Sigma\Sigma|I_{hi} - \langle I \rangle|/\Sigma\Sigma I_{hi}$.

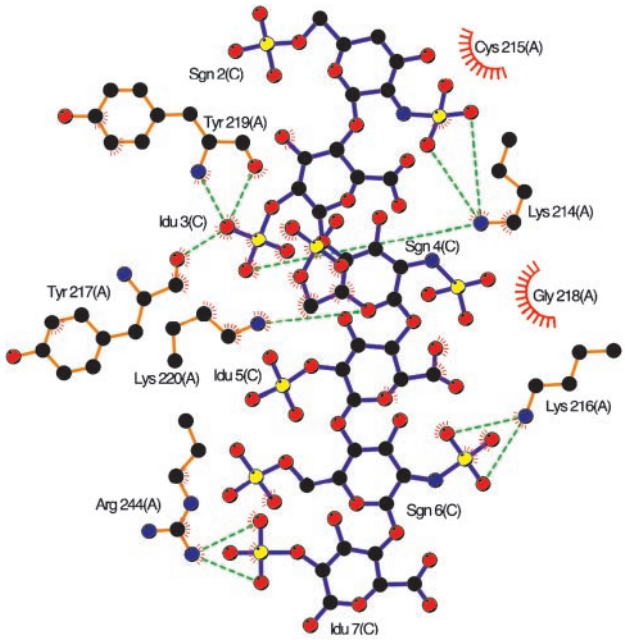

Fig. 1. VCP–heparin interactions. LIGPLOT (40) representation of VCP–heparin interaction (VCP-A/hepC). Heparin bonds are colored purple; protein bonds, gold. Carbon atoms are colored black, oxygen is red, nitrogen is blue, and sulfur is yellow. Hydrogen bonds are shown as dashed green lines, and hydrophobic contacts are shown as semicircle with lines.

to its function as a complement regulator and may have potential implications for the functioning of other complement regulators. In addition, the protein–carbohydrate contacts observed in the complex might constitute a model for such interactions in other complement regulators and contribute to understanding the structural biology of complement-related diseases such as HUS.

Materials and Methods

Crystallization. Expression (22) and purification (19) of VCP have been reported. Heparin fragments were purchased from Neoparin (San Leandro, CA). Crystals of complexes were obtained by the vapor diffusion method at 20°C. The reservoir solutions for the heparin decamer complex contained 200 mM Tris·HCl, pH 7.4; 100 mM NaCl; 2 mM $NiCl_2$; 0.2% β-octyl glucoside; and 14% polyethylene glycol 3350. The 4-μl droplets, placed on cover slips, were made from 2 μl of 600 μM VCP combined with 1.2 molar ratio of the heparin decamer, incubated at 4°C for 30 min and mixed with equal volumes of reservoir solutions. Incubations were performed in buffers containing 10 mM Tris·HCl, pH 7.4; 100 mM NaCl; and 0.02% NaN_3.

Data Measurement and Processing. Data were measured on the South East Regional Collaborative Access Team beam line at the Advanced Photon Source, using a MAR Research (Hamburg) charge-coupled device at 0.9791 Å. All measurements were made on flash-frozen crystals at 100 K. HKL2000 (31) was used for processing and scaling. Crystallographic parameters are given in Table 1.

Structure Solution and Refinement. The structure was determined through molecular replacement by using BEAST (32) as implemented in CCP4 (33). The first three SCRs of native VCP (19) were used as the search model. Initial models, built with O (34) into density modified flattened maps (35), were refined by using CNS (36) with all measured data to 2.1 Å. A mask-based model, implemented in CNS, was used for the unordered solvent. Cross-validation was performed through free R values (37) by using 5% of the reflections chosen randomly to span the resolution range; a summary is presented in Table 1. Separate noncrystallographic symmetry transformations for the protein and carbohydrate were calculated from initial atomic models and equivalent atomic coordinates and B factors restrained; weights for the restraints were chosen to minimize R_{free}. Residue R7 in chain B of VCP does not have density for atoms beyond Cγ. No density is present for the last disaccharide in both copies of heparin. In the first disaccharide in chain C, atoms C4, C5, C6, O, O61, O62, and O1 are not visible, whereas only O1 of the corresponding residue in chain D is not visible. Because HPLC analysis of the material from dissolved crystals showed the carbohydrate to be a decamer, the ends are probably disordered in the crystals. Density for OT in R244 is not present in either VCP molecule, and P237 in both chains adopts the cis conformation, as it does in native VCP. The program DYNDOM (38) was used for analysis of the hinge bending motion. Solvent accessibility calculations used a 1.4-Å probe sphere. Figs. 2 and 5 were made by using RIBBONS (39); Fig. 1 was made by using LIGPLOT (40) and Fig. 6, by using GRASP (41). The sequence numbering adopted for FH is that for the mature polypeptide. Coordinates (1RID) and structure factors (R1RIDSF) have been deposited in the Protein Data Bank (www.pdb.org).

Results and Discussion

Structure of the Complex and VCP–Heparin Interactions. The two copies (VCP-A/hepC and VCP-B/hepD) of the complex in the asymmetric unit are nearly identical with rms deviations of 0.68 Å for VCP (all atoms excluding Arg-7), 0.27 Å (main chain atoms), 0.98 Å (side chain atoms), and 1.08 Å for all heparin atoms, excluding Idu 2. Each SCR adopts a six-stranded β-sheet topology observed in many SCR-containing proteins, including native VCP (19). Relative orientations of SCR1–3 are comparable to those in native VCP, with tilt, twist, and skew angles (ref. 42; native values in parentheses) of 65 (65), 2 (3), −78 (−76) and 62 (64), 30 (35), 110 (107), respectively, for one to two and two to three pairs; values for the SCR3–4 pair, 126 (99), 31 (3), −51 (−37), however, differ significantly, indicating substantial relative movement. Analysis using DYNDOM (38) shows that the motion is a 29.5° rotation of SCR4 about a hinge formed by residues 183 and 184, which are part of the linker (residues

BIOPHYSICS

183–187) between SCR3–4. This change results in a closer association of SCR4 with SCR3, with additional contacts made by residues D209, V211, S227, and T228 that are part of a loop in SCR4, with residues G165, N166, and S167 in SCR3. There is a nearly 200-Å^2 (22%) increase in the surface area inaccessible to solvent in the complex. A small deformation of a part of SCR4 prevents atoms in their new position, in this region of SCR4, from making close contacts with SCR3. Although the 58 common Cα atoms in SCR4, between the native and complex, can be superimposed with an rms deviation of 1.5 Å, α carbons of residues D209-V211 and S226-T228 show, respectively, rms deviations of 3.4 and 3.0 Å from their respective positions in the native structure. Significant main-chain motion in SCR3 is limited to α carbons of N166 and S167, which move by 2.7 and 2.9 Å, respectively. The six completely modeled residues of the two heparin decamers are quite similar to the helical structures observed in other heparin complexes (43), with the D-glucose amine residues adopting the favorable $^4C_1$ chair conformation (44). Among the iduronic acid residues, only that at the nonreducing end is in the $^2S_4$ skew boat conformation, whereas the rest are in the ^2S_o conformation.

Interactions between heparin and VCP in the complex are electrostatically anchored by three lysines, 214, 216, and 220, along with the C-terminal R244, shown for VCP-A/hepC in Fig. 1. A representative section of the experimental electron density map contoured around heparin and LIGPLOT of VCP C/heparin D are published as supporting information on the PNAS web site. VCP A makes a total of 11 electrostatic contacts with hepC, whereas VCP B makes a total of nine electrostatic contacts with hepD. Although both Y217 and Y219 make electrostatic interactions in both copies, in VCP-A/hepC, the interaction is through main-chain carboxy atoms, whereas in VCP-B/hepD, the sidechain hydroxyl provides the contacts. In addition, van der Waals contacts with heparin are made by other sidechain atoms of the four basic residues as well as C215, Y217, G218, and Y219 in VCP-A/hepC and Y217, G218, and Y219 in VCP-B/hepD. This mix of electrostatic and van der Waals interactions parallels those observed in similar complexes (43). The SCR4–heparin interaction buries 856 Å^2 of solvent-accessible surface area in copy A and 907 Å^2 in copy B.

Heparin-mediated processes are ubiquitous in biological systems, ranging from modulation of serine protease activity to playing a prominent role in signal transduction by many growth factors. Four broad structural classes have been described in heparin interaction with proteins. The first, typified by antithrombin, causes significant changes in protein structure; heparin tetrasaccharides make two different kinds of interactions with annexin V, one involving both N and O sulfo groups and the other only the latter; the heparin-binding site in foot and mouth disease virus is composed of ligands contributed from three different viral polypeptides, VP1–3 (all reviewed in ref. 45). Fourth, FGFs are among the most extensively studied heparin-binding proteins, and structures of several FGFs and their complexes with heparin and FGF receptors have led to models for signal transduction through tyrosine kinase receptors (reviewed in ref. 46). Although heparin binding by complement regulators is functionally unrelated to FGFs, there are geometric similarities in interactions made by both classes of proteins with heparin, largely due to the dominant involvement of basic sidechains on the proteins (43). We had earlier used the structure of FGF1 (24) to propose a model for heparin binding by ^{VCP}SCR4, with Lys-214, -216, -220, and -241 as ligands (19). Lys-241 and Arg-244 are spatially close, and either could ligand heparin. This structure, however, shows that Arg-244, disordered in the native structure, is preferred.

Possible Implications for Complement Regulation. Both our modeling studies (19) and binding studies using deletion mutants of VCP (5) had suggested that specific heparin binding was a property confined to SCR4; the structure of this complex reinforces that conclusion. Unliganded VCP has a nearly invariant conformation, as evidenced by the five crystallographically independent copies in the two native structures (19). Similarly, the pair of VCP molecules in the asymmetric unit of the heparin complex show a nearly identical conformational change from native VCP. Binding sites for C3b and C4b are spread over three or more SCRs in complement regulators, making relative orientations of modules important for maintaining appropriate alignment of interacting residues (47). Although the structure of native VCP shows that there are significantly populated rigid conformations of the molecule, experimental studies, including NMR and calorimetric and fluorescence spectroscopic measurements, have been used to show significant flexibility between SCRs in MCP, VCP, FH, DAF, and CR1 (13, 16). Mobility between SCR domains has also been suggested as the structural underpinning for conformational transitions that are likely be triggered by ligand binding in complement regulators, including VCP, FH, and several others (16, 19, 48). Interaction with heparin is not essential for binding of VCP to C3b/C4b (1), because it is not for FH (25) or C4BP (49). Because the only major difference between the heparin bound and free conformations of VCP is the motion about the hinge between SCR3–4, and significant spontaneous flexibility at SCR junctions is possible, the heparin-bound conformation might likely be accessible to VCP in the course of its normal molecular dynamics. It is thus probable that heparin binding has stabilized a conformation previously accessible to the protein and might represent one of several that NMR studies have identified.

Several pieces of evidence have been used to identify potential contact points on VCP for C3b/C4b. The native structure allowed us (19), using mutational data on MCP (50) and sequence conservation between the two, to suggest that the putative C3b contacting surface is constructed with contributions from some or all of residues R7, K12, K14, R40, K41, K43, K50, K64, R65, and R66, which form a positive patch at the junction of SCR1–2, along with residues E102 (in SCR2) and K186 and H189 (near the N terminus of SCR4). Similarly, we had identified N94, H98, and E102 as possible contact points for C4b. Observations made on the smallpox inhibitor of complement enzymes (SPICE), the *variola* analog of VCP, which differs in 12 residues from VCP, support these inferences. The nearly 100-fold greater potency of SPICE relative to VCP has been attributed to changes in residues that are suggested contact points between VCP and C3b/C4b. A ^{VCP}E120K change in SPICE is identical to the alteration made in SCR2 of CR1 that enhances the latter's C3b-binding and cofactor activity. Similarly, the ^{VCP}H98Y mutation in SPICE brings the latter's sequence closer to that of the region in MCP identified as interacting with both C3b and C4b and might be a second major contributor (51). It is clear from Fig. 2 that binding of heparin to SCR4 significantly changes the relative separation and orientation of residues K186, H189, F201, and R203 with respect to N94, H98, E102, and E108. This change might have a direct effect on VCP interaction with C3b and C4b, because all these residues, except F201, are expected to contact C3b/C4b. The changes range from a low of 0.8 Å between Cα atoms of K186 and E102 in the native compared to those in the heparin complex to a high of 6 Å between H189 and H98 Cα atoms in the two structures. Similarly, the distance between the centroid of the positive patch residues at the junction of SCR1–2 and residues K186, H189, F201, and R203 also change by 0.4, 4.0, 4.5, and 1.1 Å, respectively, in the complex. Binding of heparin at the bottom of SCR4 promotes a closer association of SCR3–4. The buried surface area between SCR3–4 in the heparin complex is 1,045 Å^2 compared to 859 Å^2 in the native structure, a 22% increase, making the altered orientation marginally more stable. Although

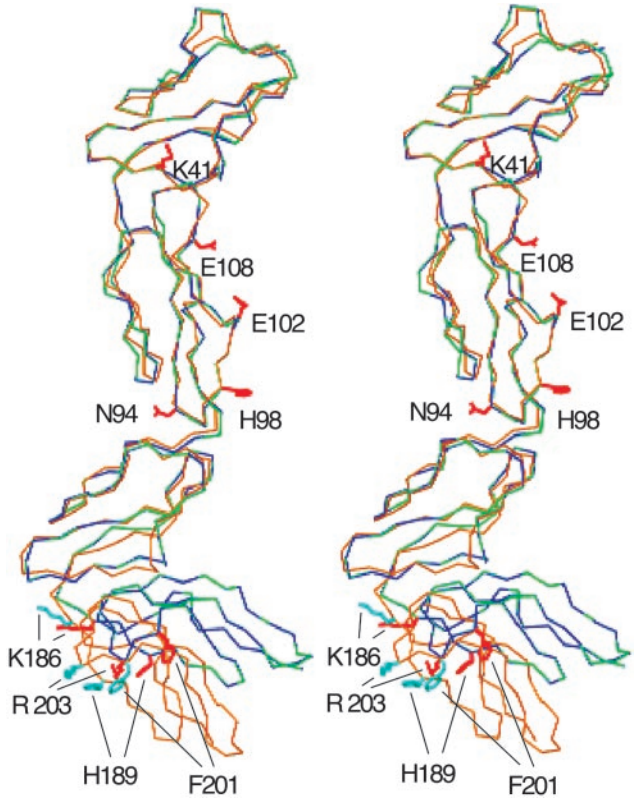

Fig. 2. Conformational change. The four SCRs of VCP-A/hepC (green), VCP-B/hepD (blue) are superimposed on those of native VCP (gold). Sidechains that might contact C3b/C4b in the native (cyan) and heparin-bound (red) conformations are also shown.

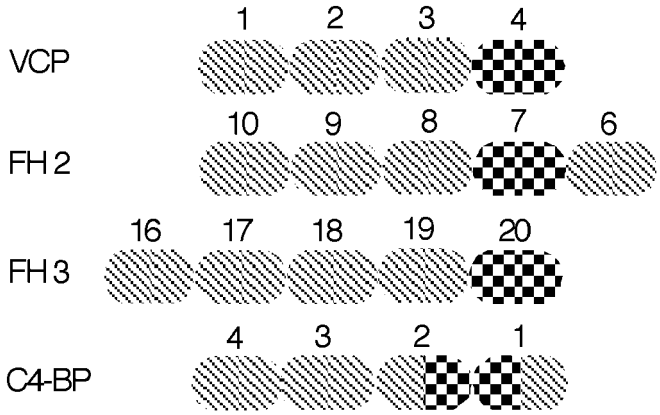

Fig. 3. Heparin binding relative to C3b binding. Each SCR is shown as an oval, cross hatched to show C3b binding and checkered to show heparin binding. FH2 and FH3 are the second and third C3b-binding sites in FH, with their associated heparin sites. Only the first four SCRs of C4b-BP of the α chain are shown. SCRs are numbered to show the polypeptide chain direction.

the increase in solvent-accessible area lost is not large, the new conformation is stabilized by the much larger area lost through interaction with heparin at the distal end of SCR4. The heparin-stabilized change in conformation might consequently affect the kinetics and dynamics of VCP interactions with C3b/C4b by varying the relative positions of residues that participate in the interaction.

In contrast to the classical pathway, the alternative pathway of complement activation makes a distinction between host and target unaided by antibodies. The central role in this process is played by the interaction of FH with heparin, sialic acid, and other polyanions on host cell surfaces, activation being strongly down-modulated on such anionic surfaces. It has been proposed that differing affinities of the heparin-binding sites on FH for polyanions of different structure and charge distribution, such as heparin and sialic acid, enable it to vary its residence times on different cellular surfaces. Combined with its multiple C3b-binding sites and flexibility at its 19 SCR junctions, this results in a variation of the duration and intensity of complement activation on diverse cell surfaces, contributing to its remarkable host-target discrimination power. The multimeric C4BP also possesses multiple C4b and heparin-binding sites on its eight α chains but regulates the classical pathway. VCP, on the other hand, has binding sites for both C3b and C4b and a single heparin-binding site and regulates both pathways. It thus shares structural and functional characteristics with both FH and C4BP (3, 5, 19).

The structural and functional similarities among VCP, FH, and C4BP have been attributed to their evolutionary origin. Comparison of amino acid sequences between SCRs within a molecule and those between SCRs of different molecules has been used to suggest that an ancestor of both FH and C4BP arose through repeated gene duplications. FH and C4BP diverged from this ancestral molecule, with FH having appeared significantly earlier (52). Furthermore, VCP is regarded as the evolutionarily altered product of a complement regulator originally acquired by vaccinia from a human host (53). Structural information comparable to that on VCP is currently unavailable for FH and C4BP; existing data, however, show that in both FH and C4BP, the heparin-binding sites are located in close proximity to the C3b/C4b-binding sites, as they are in VCP, and the relative spatial dispositions of the sites are preserved (Fig. 3). There are three C3b-binding sites in FH, each interacting with a different region of C3b (54, 55): an N-terminal site that is responsible for decay acceleration and factor I cofactor activity, mapped to SCR1–4, and two others mapped to SCR6–10 (FH2 in Fig. 3) and SCR16–20 (FH3), respectively (25). Three heparin-binding sites have also been identified on FH, one each on SCR7, -13, and -20 (20, 21). The heparin-binding site on SCR20 is on the most C-terminal of the five SCR set 16–20, which constitutes the third C3b site on FH; this location is similar to that in SCR4 of VCP, relative to the C3b interaction sites on the latter (Figs. 2 and 3). The heparin-binding site on SCR7 in FH is on the penultimate N-terminal SCR of the group of five that form the second C3b-binding site, a topologically analogous location to that in VCP. The heparin-binding site on SCR13 does not conform to this plan; its physiological function, however, is currently considered uncertain (56), and it is not included in Fig. 3. The location of the heparin-binding site in C4BP at the junction of SCR1–2 of each α chain, with the C4b interactions occurring with SCR1–4 (49), is again similar in relative positioning to that in VCP, FH2, and FH3. Thus the topological relation of C3b to heparin-binding SCRs appears to have been evolutionarily preserved, perhaps because it is one simple and effective way to enable polyanion binding to modulate interactions with C3b/C4b, through relative SCR movements.

Although there are no currently available experimental data for heparin modulation of the complement regulatory activity in VCP, effects of polyanions on the activity of FH have been well documented (25, 57). Structural and biophysical studies have indicated the presence of significant mobility at SCR junctions in fragments of VCP and FH (13, 58). Electron microscopic (59) and solution x-ray scattering (48) studies of full-length FH have also implied flexibility that result in a folded-back structure. In addition, it has been proposed, based on the solution structure of FH, that heparin binding might allow for a reconfiguration of C3b-binding sites in FH by altering relative SCR orientations (48). Thus the hinge bending

```
                 .          .  .   .  . . ..   . ... .. ..... .     ..  .     . . ...
VCP     186 KCPHPT..ISNGYISSGF..K.RSYS.YNDNVDFKCKYGYKLSGSS...SSTCSPGNTWKPELPKCVR.
H-FH   1148 PCVISREIMENYNIALRWTAKQKLYSRTGESVEFVCKRGYRLSSRSHTLRTTCWDG.KL..EYPTCAKR
                            **    * *  *  *          *    *
```

Fig. 4. Sequence comparison. The sequence correspondence between ^{FH}SCR20 and ^{VCP}SCR4 is shown. Identical or conservative replacements are indicated by a period. Basic residues that are ligands to heparin in the VCP/heparin complex or in the modeled ^{FH}SCR20/heparin complex are colored red. Mutations in ^{FH}SCR20 that have been characterized in HUS patients are shown by asterisks.

that we observe in the VCP/heparin structure might indicate a potential mechanistic means that is also available to the other fluid-phase regulators, FH and C4BP.

Potential Relevance to HUS. HUS is a family of diseases characterized by thrombocytopenia and hemolytic anemia, frequently resulting in renal failure, especially in children. The nondiarrhea-associated form, termed atypical or familial HUS, is caused by mutations in the FH gene, resulting in functional deficiencies in FH. Mutation of nine residues in ^{FH}SCR20 of HUS patients has been identified by genetic studies (27) as important for binding heparin. A modeling study (28) has proposed FH residues R1164, K1168, K1170, and R1174 in SCR20 as electrostatic ligands. However, as observed in another recent study (29), although these residues are conserved between FH and the FH-related proteins FHR3 and FHR4, the latter has no heparin-binding activity. The experimentally observed position of heparin in this VCP/heparin complex can be used to suggest an analogous location in FH and to demonstrate a better correlation between heparin binding and HUS mutations. The sequence correspondence that follows as a corollary to the structural equivalencies between the β strands in ^{VCP}SCR4 and an ^{FH}SCR20 model based on it (28) is shown in Fig. 4. The alignment makes 28 residues identical or conservatively substituted between ^{VCP}SCR4 and ^{FH}SCR20, including (FH residues in parentheses) K216 (K1184), K220 (R1188), and K244 (K1212), three of the four basic residues that anchor VCP interaction with heparin (Fig. 1). In the previous modeling study (28), a basic patch identified in ^{FH}SCR20 included six residues, K1184, R1185, R1188, R1192, K1212, and R1213, none of which were considered as heparin ligands, because they were not conserved across species. However, as shown in Fig. 5, when ^{FH}SCR20 is superimposed over ^{VCP}SCR4, all six residues of the basic patch, in addition to R1164 and R1197, are within liganding distance of the experimentally determined position of heparin in VCP. It is interesting that the noncorresponding residue in the quartet of VCP heparin ligands is K214. SPICE, the *variola* analog of VCP, incorporates a K214T mutation and yet binds to heparin columns as strongly as VCP (60). However, Thr is also often found as a ligand to heparin (24, 43) and is frequently observed as the replacement for one of the basic heparin ligands (61). In addition, there are other basic residues that are spatially close to K214 that could potentially interact with heparin in its absence. Finding R1192 and R1197 in the list of potential ligands is significant; of the nine substitution mutations in ^{FH}SCR20 observed in HUS patients, only two are of basic residues, R1192C and R1197G/Q. The other potential heparin ligands in our model, R1185, R1188, R1192, K1212, and R1213, are also precisely those determined (29) to affect both C3d and heparin binding by a human ^{FH}SCR15–20 construct.

The majority of the nine residues mutated in ^{FH}SCR20 from HUS are not basic residues (Fig. 4). Although some of them might contact C3b directly, the VCP/heparin structure suggests that some residues in complement regulators might be important in maintaining the inter-SCR flexibility and orientation necessary for interaction with ligands. Residues 206–211 in ^{VCP}SCR4 form part of the region that stabilizes the new conformation that SCR4 adopts by van der Waals interactions with residues 163–168 of SCR3. Mutation of these residues is likely to result in a significant alteration of the geometric nature and extent of this conformational change, which would lead to different spatial arrangement of residues likely to interact with C3b/C4b. Three of the substitutions of nonbasic residues associated with HUS (corresponding residues in VCP in parentheses), S1173L(S206) G1176D(N208), and V1179A(V211), are precisely in an analogous region of ^{FH}SCR20 (Fig. 6). The sequence of residues in this region is likely to have been evolutionarily optimized to match the geometric nature and range of motion required for function, independently in each molecule. Changes to the native sequence are likely to lead to alterations in direction, plasticity, and extent of motion previously accessible, which could directly affect

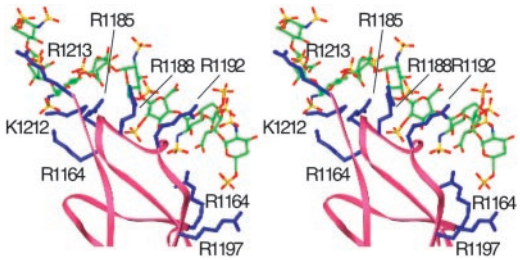

Fig. 5. ^{FH}SCR20 binding to heparin. A stereo pair of the modeled ^{FH}SCR20/heparin complex. Main-chain trace of SCR20 is shown in pink. The six basic residues that are within liganding distance of heparin are shown in blue, with sidechain positions modeled from the corresponding VCP residue. The heparin model is derived from that in this structure by extending the reducing end by one repeating unit, using the helical parameters of the experimental structure. Carbon atoms are colored green, oxygens are red, nitrogens are blue, and sulfurs are yellow.

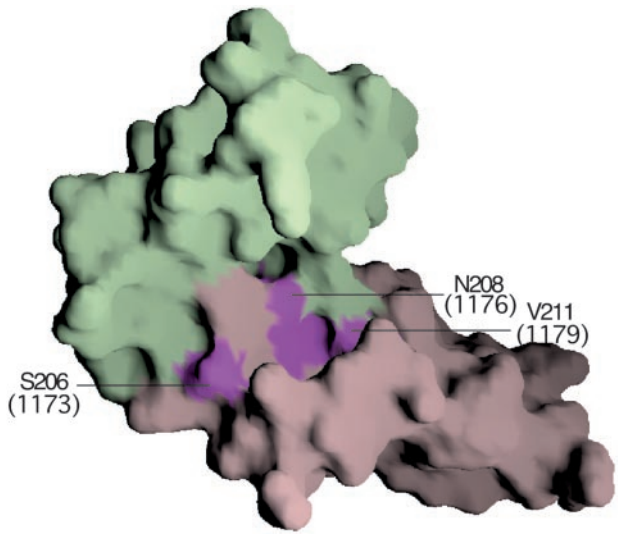

Fig. 6. Residues that delimit motion. A surface representation of VCP SCR3 (light green) and SCR4 (light purple) is shown. Surface patches of residues, the mutation of which might result in altered motion, are colored magenta, with corresponding numbers of FH residues (Fig. 4) in parentheses.

function, for example, by stabilizing a conformation that leads to a spatial distribution of C3b contacting residues significantly different from that in the native structure.

We thank J. Chrzas for help with data measurement at the South East Regional Collaborative Access Team (ID22) at the Advanced Photon Source, Chicago, supported by the U.S. Department of Energy, Basic Energy Sciences. We also thank Larry DeLucas for support, Ken Judge for technical assistance, M. Suresh Kumar for help with data measurement, and S. V. L. Narayana for previewing the manuscript. This research is supported by National Institutes of Health Grant AI51615 (to K.H.M.M.) and by partial funding from the Jewish Hospital Research. G.J.K. is a Senior Wellcome Trust Fellow in South Africa.

1. Kotwal, G. J. & Moss, B. (1988) *Nature* **335,** 176–178.
2. Kotwal, G. J. (2000) *Immunol. Today* **21,** 243–248.
3. Kotwal, G. J., Issacs, S. T., McKenzie, R., Frank, M. M. & Moss, B. (1990) *Science* **250,** 827–830.
4. Rosengard, A. M., Alnonso, L. C., Korb, L. C., Baldwin, W. M., Sanfilippo, F., Turka, L. A. & Ahearn, J. M. (1999) *Mol. Immunol.* **36,** 685–697.
5. Smith, S. A., Sreenivasan, R., Krishnasamy, G., Judge, K. W., Murthy, K. H., Arjunwadkar, S. J., Pugh, D. R. & Kotwal, G. J. (2003) *Biochim. Biophys. Acta* **1650,** 30–39.
6. Fearon, D. T. & Locksley, R. M. (1996) *Science* **272,** 50–53.
7. Cooper, N. R. (1991) *Immunol. Today* **12,** 327–331.
8. Makrides, S. C. (1998) *Pharmacol. Rev.* **50,** 59–87.
9. Smith, S. A., Krishnasamy, G., Murthy, K. H., Cooper, A., Bromek, K., Barlow, P. N. & Kotwal, G. J. (2002) *Biochim. Biophys. Acta* **1598,** 55–64.
10. Bork, P., Downing, A. K., Kieffer, B. & Campbell, I. D. (1995) *Q. Rev. Biophys.* **29,** 119–167.
11. Pangburn, M. K. & Muller-Eberhard, H. J. (1983) *Biochemistry* **22,** 178–185.
12. Dahlback, B., Smith, C. A. & Muller-Eberhard, H. J. (1983) *Proc. Natl. Acad. Sci. USA* **80,** 3461–3465.
13. Kirkitadze, M. D. & Barlow, P. N. (2001) *Immunol. Rev.* **180,** 146–161.
14. Casasnovas, J. M., Larvie, M. & Stehle, T. (1999) *EMBO J.* **18,** 2911–2922.
15. Smith, B. O., Mallin, R. L., Krych-Goldberg, M., Wang, X., Hauhart, R. E., Bromek, K., Uhrin, D., Atkinson, J. P. & Barlow, P. N. (2002) *Cell* **108,** 769–780.
16. Uhrinova, S., Lin, F., Ball, G., Bromek, K., Uhrin, D., Medof, M. E. & Barlow, P. N. (2003) *Proc. Natl. Acad. Sci. USA* **100,** 4718–4723.
17. Gaboriad, C. G., Bally, I., Arlaud, G. J. & Fonticella-Camps, J. C. (2000) *EMBO J.* **19,** 1755–1765.
18. Szakonyi, G., Guthridge, J. M., Li, D., Young, K., Holers, V. M. & Chen, X. S. (2001) *Science* **292,** 1725–1728.
19. Krishna Murthy, H. M., Smith, S. A., Ganesh, V. K., Judge, K. W., Mullin, N., Barlow, P. N., Ogata, C. O. & Kotwal, G. J. (2001) *Cell* **104,** 301–311.
20. Pangburn, M. K., Atkinson, M. A. L. & Meri, S. (1991) *J. Biol. Chem.* **266,** 16847–16853.
21. Blackmore, T. K., Hellwage, J., Sadlon, T. A., Higgs, N., Zipfel, P. F., Ward, H. M. & Gordon, D. L. (1998) *J. Immunol.* **160,** 3342–3348.
22. Smith, S. A., Mullin, N. P., Parkinson, J., Shchelkunov, S. N., Totmentin, A. V., Loparev, V. N., Srisatjaluk, R., Reynolds, D. N., Keeling, K. L., Justus, D. E., *et al.* (2000) *J. Virol.* **74,** 5659–5666.
23. Al-Mohanna, Parhar, R. & Kotwal, G. J. (2000) *Transplantation* **71,** 796–801.
24. Schlessinger, J., Plotnikov, A. N., Ibrahimi, O. A., Eliseenkova, A. V., Yeh, B. K., Yayon, A., Linhardt, R. J. & Mohammadi, M. (2000) *Mol. Cell* **6,** 743–750.
25. Pangburn, M. K., Pangburn, K. L. W., Koistinen, V., Meri, S. & Sharma, A. K. (2000) *J. Immunol.* **164,** 4742–4751.
26. Richards, A., Goodship, J. A. & Goodship, T. H. (2002) *Curr. Opin. Nephrol. Hypertens.* **11,** 431–435.
27. Zipfel, P. F., Skerka, C., Caprioli, J., Manuelian, T., Neumann, H. H., Noris, M. & Remuzzi, G. (2001) *Int. Immunopharmacol.* **1,** 461–468.
28. Perkins, S. J. & Goodship, T. H. (2002) *J. Mol. Biol.* **316,** 217–224.
29. Hellwage, J., Jokiranta, T. S., Friese, M. A., Wolk, T. U., Kampen, E., Zipfel, P. F. & Meri, S. (2002) *J. Immunol.* **169,** 6935–6944.
30. Giannakis, E., Jokiranta, T. S., Male, D. A., Ranganathan, S., Ormsby, R. J., Fischetti, V. A., Mold, C. & Gordon, D. L. (2003) *Eur. J. Immunol.* **33,** 962–969.
31. Otwinowski, Z. & Minor, W. (1997) in *Methods in Enzymology*, eds. Carter, C. W. & Sweet, R. M. (Academic, New York), Vol. 276, pp. 307–326.
32. Read, R. J. (2001) *Acta Crystallogr. D* **57,** 1373–1382.
33. CCP4 (1993) *Acta Crystallogr. D* **50,** 760–763.
34. Jones, T. A., Zou, J. Y., Cowans, S. W. & Kjeldgaard, M. (1991) *Acta Crystallogr. A* **47,** 110–119.
35. Cowtan, K. D. & Zhang, K. Y. (1999) *Prog. Biophys. Mol. Biol.* **72,** 245–270.
36. Brunger, A. T., Adams, P. D., Clare, G. M., Gross, D., Grosse-Kunstleve, R. W., Jiang, J.-S., Kuszewski, J., Nilges, M., Pannu, N. S., Read, R. J., *et al.* (1998) *Acta Crystallogr. D* **54,** 905–921.
37. Brunger, A. T. (1992) *Nature* **355,** 472–475.
38. Hayward, S. & Berendsen, H. J. (1998) *Proteins* **30,** 144–154.
39. Carson, M. C. (1997) in *Methods in Enzymology*, eds. Carter, C. W. & Sweet, R. M. (Elsevier, New York), Vol. 277B, pp. 493–505.
40. Wallace, A. C., Laskowski, R. A. & Thornton, J. M. (1995) *Protein Eng.* **8,** 127–134.
41. Nicholls, A., Sharp, K. A. & Honig, B. (1991) *Proteins Struct. Funct. Genet.* **11,** 281–289.
42. Wiles, A. P., Shah, G., Bright, J., Perczel, A., Campbell, I. D. & Barlow, P. (1997) *J. Mol. Biol.* **272,** 253–265.
43. Raman, R., Venkataraman, G., Ernst, S., Sasisekharan, V. & Sasisekharan, R. (2003) *Proc. Natl. Acad. Sci. USA* **100,** 2357–2362.
44. IUPAC. (1981) *Arch. Biochem. Biophys.* **207,** 469–472.
45. Mulloy, B. & Linhardt, R. J. (2001) *Curr. Opin. Struct. Biol.* **11,** 623–628.
46. Pellegrini, L. (2001) *Curr. Opin. Struct. Biol.* **11,** 629–634.
47. Krych, M., Hauhart, R. & Atkinson, J. P. (1998) *J. Biol. Chem.* **273,** 8623–8629.
48. Aslam, M. & Perkins, S. J. (2001) *J. Mol. Biol.* **309,** 1117–1138.
49. Blom, A. M., Webb, J., Villoutreix, B. O. & Dahlback, B. (1999) *J. Biol. Chem.* **274,** 19237–19245.
50. Liszewski, M. K., Leung, M., Cui, W., Subramanian, V. B., Parkinson, J., Barlow, P. N., Manchester, M. & Atkinson, J. P. (2000) *J. Biol. Chem.* **275,** 37692–37701.
51. Rosengard, A. M., Liu, Y., Nie, Z. & Jimenez, R. (2002) *Proc. Natl. Acad. Sci. USA* **99,** 8808–8813.
52. Krushkal, J., Bat, O. & Gigli, I. (2000) *Mol. Biol. Evol.* **17,** 1718–1730.
53. Rosengard, A. M. & Ahearn, J. M. (1999) *Immunopharmacology* **42,** 99–106.
54. Sharma, A. K. & Pangburn, M. K. (1996) *Proc. Natl. Acad. Sci. USA* **93,** 10996–11001.
55. Jokiranta, T. S., Hellwage, J., Koistenen, V., Zipfel, P. F. & Meri, S. (2000) *J. Biol. Chem.* **275,** 27657–27662.
56. Blackmore, T. K., Sadlon, T. A., Ward, H. M., Lublin, D. M. & Gordon, D. L. (1996) *J. Immunol.* **157,** 5422–5427.
57. Meri, S. & Pangburn, M. K. (1990) *Proc. Natl. Acad. Sci. USA* **87,** 3982–3986.
58. Henderson, C. E., Bromek, K., Mullin, N. P., Smith, B. O., Uhrin, D. & Barlow, P. N. (2000) *J. Mol. Biol.* **307,** 323–339.
59. Di Scippio, R. G. (1993) *Cell* **149,** 2592–2599.
60. Dunlop, L. R., Oehlberg, K. A., Reid, J. J., Avci, D. & Rosengard, A. M. (2003) *Microbes Infect.* **5,** 1049–1056.
61. Faham, S., Hileman, R. E., Fromm, J. R., Linhardt, R. J. & Rees, D. C. (1996) *Science* **271,** 1116–1120.